Removal of Per- and Polyfluoroalkyl Substances (PFASs) from Contaminated Groundwater using Granular Activated Carbon: A Pilot-Scale Study with Breakthrough Modeling

Charlie J. Liu[a], David Werner[b], and Christopher Bellona[a*]

[a] Department of Civil and Environmental Engineering, Colorado School of Mines, Golden, Colorado 80401, United States

[b] School of Engineering, Newcastle University, Newcastle upon Tyne, England, United Kingdom

*** Corresponding author**:

Christopher Bellona

303-273-3061

cbellona@mines.edu

Environmental Science: Water Research and Technology

Table of Contents Entry

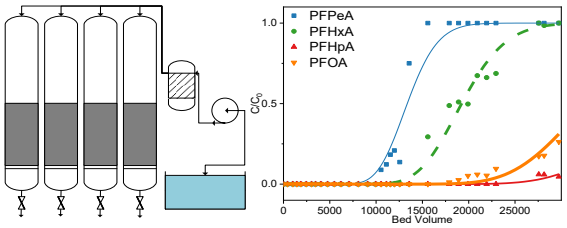

Pilot-scale treatment of PFAS contaminated groundwater with GAC; chain length dependent breakthrough; better PFAS adsorption correlated with more GAC transport pores; breakthrough modeling

Abstract

Granular activated carbon (GAC) is a commonly used technology for removal of per- and polyfluoroalkyl substances (PFAS). However, most studies characterizing PFAS absorption to GAC are performed in small bench-scale tests with synthetic groundwater, which poorly approximates conditions encountered in full-scale treatment systems. Pilot-scale studies, although somewhat rare, better predict full-scale performance due to realistic operating conditions. This study presents breakthrough results from a pilot-scale GAC system operated for seven months treating a continuous source of PFAS contaminated groundwater with four activated carbons, Calgon F400 and F600, and Norit GAC400 and GCN1240. Chain length dependent breakthrough was generally observed for perfluorocarboxylates (PFCAs) and perfluorosulfonates (PFSAs) where shorter chain PFASs broke through faster than longer chain PFASs. All tested GACs performed similarly for weakly adsorbing shorter chain PFASs, suggesting that GAC properties may not affect breakthrough for these PFASs. However, F400 and GAC400 performed 40-50% better than F600 and GCN1240 for strongly adsorbing long chain PFASs, which may be due to a higher volume of transport pores within F400 and GAC400. Breakthrough curves were fit by equilibrium and intraparticle diffusion models using the solid liquid partition coefficient (K_d). The

equilibrium model was found to be a better fit for the data and a more practical model. Model K_d outputs from the pilot study were compared against a separate batch study. Comparisons showed that batch study K_d values were larger for longer chain compounds and smaller for shorter chain compounds.

Water Impact Statement:

Per- and polyfluoroalkyl substances (PFASs) are recalcitrant compounds harmful to human health and are often treated by granular activated carbon (GAC). Pilot-scale systems may more accurately represent full-scale performance than lab-scale systems. Better adsorption was found for longer chained PFASs and GACs containing more transport pores. Breakthrough curves were model fitted and may provide breakthrough insights for other treatment systems.

1.0 Introduction

Widespread use of per- and polyfluoroalkyl substances (PFASs) in industrial and firefighting applications with aqueous film forming foams (AFFFs) has resulted in the detection of PFASs in soil, water, and human blood samples worldwide[1-7]. Once released, PFASs are persistent in the environment primarily due to the strength of the C-F bond at 441 kJ/mol[8]. PFASs are toxic to human health and have been implicated in developmental effects, liver toxicity, cancer, immune system impacts, and other health effects[9-12]. As a result, the U.S. Environmental Protection Agency (USEPA) issued life-time health advisories for two PFASs, perfluorooctanoic acid (PFOA) and perfluorooctane sulfonate (PFOS) at 70 ng/L individually or combined[9, 10].

Remediation technologies for PFASs involve destructive technologies such as electrochemical, plasma, and UV processes[13-15], separation technologies such as high-pressure membranes (i.e., nanofiltration or reverse osmosis)[16, 17], and adsorption technologies such as granular activated carbon (GAC)[18-22] and ion exchange (IX)[23-25]. Of these technologies, GAC and IX are currently widely used and accessible technologies for PFAS remediation. When GAC and IX are compared under the same experimental conditions, IX often adsorbs more PFASs than GAC[21, 24, 26]. However, many IX experiments have been performed in the absence of dissolved organic carbon (DOC) or competing anions which may affect IX adsorption performance[27]. In addition, IX generally has higher capital costs than GAC and regeneration of IX and disposal of regeneration wastes may also incur additional costs. Lastly, it is difficult to elucidate the mechanism of adsorption for many IX resins because they are proprietary[27]. As a result, GAC may still be as favorable as IX.

PFAS removal with GAC has been well-studied using small, bench-scale experiments like batch isotherm tests[19-22, 26, 28, 29] or rapid small-scale column tests (RSSCTs)[18, 24, 26]. However, there is a lack of PFAS removal data from pilot-scale GAC studies in the literature. Although there are drawbacks to pilot-scale testing such as cost and ease of operation, pilot-scale experimental conditions including feed water composition of organic contaminants and organic matter, GAC particle size, and contaminant concentration ranges are more representative of full-scale performance than batch studies or RSSCTs.

Feed water composition can significantly impact adsorption of organic contaminants with GAC. When the influent concentration of organic contaminants or DOC fluctuates, like in full-scale systems, adsorption and desorption equilibrium can also fluctuate, resulting in a dynamic

equilibrium[30-34]. DOC can significantly decrease sorption of organic contaminants due to competitive adsorption, pore blockage, reduced mass transfer surface area, and changes in film mass transfer coefficient[18, 30, 35-38]. Film mass transfer coefficient may decrease as a result of increased local fluid viscosity[36, 39, 40]. These feed water composition effects can be simulated in pilot-scale systems and RSSCTs assuming a constant flow of real contaminated groundwater. However, RSSCT results may still deviate from pilot-scale results. In studies comparing pilot-scale and RSSCT studies for trichloroethylene (TCE) removal, breakthrough occurred faster at the pilot-scale[35, 41]. As a result, scaling factors have been suggested for RSSCTs to match pilot-scale systems for removal of organic contaminants like atrazine, DEET, simazine, and prometon[35]. On the other hand, the effect of changing influent concentrations cannot be observed in batch studies where no flow occurs and static equilibrium conditions with constant concentrations exist. Isotherm parameters have been used to predict pilot-scale results with atrazine; however, a scaling factor is still necessary[36].

Particle size and distribution also have a significant impact on adsorption. In many cases, RSSCT and batch studies utilize pulverized GAC to eliminate GAC size uniformity variations because small masses are used (100 mg) and because GAC typically has high uniformity coefficients (UC = 1.5-2) used to promote stratification during backwashing[39]. GAC is also pulverized in RSSCTs to a ratio of 1:30 particle size to column diameter to prevent wall or channeling effects[39]. However, pulverized GAC is not representative of pilot- or full-scale operations, which uses unpulverized GAC. It has been demonstrated that pulverized GAC has a larger adsorption capacity than unpulverized GAC[35, 37, 39]. For example, a recent study found that sub-micron powdered activated carbon, a highly pulverized activated carbon, had an adsorption capacity for PFASs 480 times

114 larger than GAC[42]. In another study observing PFAS adsorption with an AFFF contaminated water
115 using different sieved particle sizes of the same GAC, the smallest particle size demonstrated the
116 greatest removal of PFOA and PFOS after 5 days of equilibration[20]. As GAC particles are ground
117 smaller, the available surface area exposed to the bulk flow is greater, resulting in more adsorption.
118 When DOC is present, the presence of more exposed surface area also alleviates the pore blocking
119 effects of DOC[35]. As a result, the use of pulverized GAC in RSSCT and batch studies will likely
120 overestimate breakthrough times and adsorption capacities for pilot- and full-scale adsorption
121 systems.
122
123 Lastly, batch studies and some RSSCTs generally use concentrations in the high µg/L or mg/L
124 range while concentrations practitioners or municipalities work with downstream of point source
125 contaminations are generally in the ng/L or low µg/L range[2, 6, 38, 43-45]. Because predictions outside
126 of isotherm concentration ranges should not be made, this makes batch-scale to full-scale
127 extrapolations even more difficult. In a study observing isotherm data for nonylphenol, it was
128 found that using an isotherm obtained at high concentrations to predict adsorption at a much lower
129 concentration lead to a substantial overestimation of nonylphenol removal[46].
130
131 The lack of PFAS breakthrough data representative of full-scale GAC performance was addressed
132 in this study with a pilot-scale GAC system operated for 7 months treating a continuous source of
133 real PFAS-contaminated groundwater. In addition, four different virgin, unpulverized GACs were
134 tested and compared against each other. Pilot-scale data was then fit by two models: an
135 instantaneous equilibrium model and an intraparticle diffusion model. This study provides new
136 insight into the use of GAC for PFAS removal in pilot-scale systems with real contaminated

groundwaters, which will provide guidance for assessing PFAS breakthrough for future academic studies, practitioners, and regulators.

2.0 Materials and Methods

2.1 Pilot System Operation

An automated pilot-scale system was constructed to compare four commercially available granular activated carbons. The system was deployed at a PFAS-contaminated wellhead at a city in Colorado. AFFF was assumed to be the primary source of PFAS contamination due to the proximity of firefighting training areas. Well water was fed at 2 gallons per minute (GPM), filtered through a 50 μm cartridge filter, and diverted into each column at 0.5 GPM. Flow rate through each column was regulated using automated valves, which were controlled by a supervisory control and data acquisition (SCADA) system. The GAC columns were packed to 10 minutes empty bed contact time (EBCT). The system ran for approximately 7 months or 30,000 bed volumes with 5 samples taken daily (1 influent, 4 effluent). 32 total time points were processed. Prior to operation, the GACs were soaked in deionized water for 24 hours and backwashed to 30% bed expansion. Column dimensions and a system schematic are provided in Table S1 and Figure S1 in the electronic supplementary information (ESI).

2.2 GAC Properties

Four commercially available GAC products including Filtrasorb 400 (F400) and Filtrasorb 600 (F600) from Calgon Carbon Corporation (Pittsburgh, PA) and GAC400 and GCN1240 from Cabot Norit Corporation (Boston, MA) were selected for testing. Brunauer–Emmett–Teller (BET) surface area, total pore volume, and micro, meso, and macro pore percentages were determined

using a Micrometrics TriStar II surface area and porosity analyzer (Norcross, GA). Additional parameters were provided by commercially available data sheets. GAC properties are shown in Table 1. Carbons were chosen based on differences in material, BET surface area, and pore distribution to better understand impact of carbon type on PFAS removal.

Table 1. Activated carbon physical properties

	Calgon F400	Norit GAC400	Calgon F600	Norit GCN1240
Material	Coal	Coal	Coal	Coconut
BET Surface Area (m^2/g)	785	963	614	1107
Total Pore Volume (cm^3/g)	0.27	0.30	0.16	0.21
Micropore Volume (cm^3/g)	0.05	0.05	0.03	0.09
Mesopore Volume (cm^3/g)	0.17	0.19	0.09	0.11
Macropore Volume (cm^3/g)	0.05	0.06	0.04	0.01
Iodine Number (mg/g) *	1000	1000	850	1000
Effective Size (mm) *	0.55-0.75	0.7	N/A	0.6
Apparent Density (g/mL) *	0.54	0.49	0.62	0.51
Mass in Column (kg)	10.2	11.7	9.3	9.6

* Company provided data sheet

2.3 Analytical Methods

Influent water samples were tested monthly for DOC using a Shimadzu TOC-L (Columbia, MD), major anions with ion chromatography (IC) using a Dionex ICS-90 (Sunnyvale, CA), and major

cations with inductively coupled plasma atomic emission spectroscopy (ICP-AES) using a Perkin-Elmer Optima 5300 (Fremont, CA). Primary water quality parameters include: DOC: 2.7 ± 0.6 mg/L, pH: 7.56 ± 0.4, turbidity: 0.53 ± 0.4 NTU, alkalinity: 249 ± 23.3 as $CaCO_3$, Ca: 116.3 ± 0.8 mg/L, Mg: 34.2 ± 0.2 mg/L, Na: 105.1 ± 8.6 mg/L, and S: 72.9 ± 2.3 mg/L.

All PFAS samples were collected in 15 mL pre-weighed polypropylene Falcon (Corning, NY) tubes. All reagents used in PFAS analytical methods were Fisher Scientific Optima LCMS grade (Hampton, NH) including water, methanol, isopropanol, and ammonium hydroxide. Samples were injected into a SCIEX X500R QTOF System for PFAS analysis (Framingham, MA). The analytical column used was a Phenomenex Gemini C18, 5 µm, 100 mm x 3 mm (Torrance, CA). Additional information on the PFAS sample processing method is presented in detail in the ESI. Calibration curve concentrations ranged from 0.74 ng/L to 7400 ng/L. Generally, these values represented the limits of quantification (LOQ).

2.4 Modeling

Two models were used to fit PFAS breakthrough curves using a solid liquid partition coefficient, K_d, in Matlab (MathWorks®, Inc.): an instantaneous equilibrium model and an intraparticle diffusion model[47]. Model input parameters and equations are described in detail in the ESI.

3. Results and Discussion

3.1 Breakthrough Curves

The influent water consisted of ten quantifiable PFASs with varying influent concentrations presented in Figure S2. For breakthrough analysis purposes, the influent concentration was

averaged over time as shown in Table 2. The relative abundance of various PFASs in the influent water are indicative of AFFF contamination. Relative to other compounds in the mixture, AFFF formulations generally contain very high levels of PFOS and PFHxS, high levels of PFPeA, PFHxA, and PFOA, and low levels of PFHpA, PFBS, and PFHpS[3, 20, 48]. Although at low concentrations, the relative levels of influent PFASs in the groundwater used for this study show similar trends. Breakthrough curves of C/C_0 verses bed volumes (BV), where C is the effluent concentration (ng/L) and C_0 is the average influent concentration (ng/L), are shown in Figure 1.

Table 2. Average concentrations and standard deviations of 32 influent samples over 7 months.

Compound	Abbreviation	Average Influent Concentration (ng/L)	Standard Deviation (ng/L)
Perfluoropentanoate	PFPeA	16.3	5.9
Perfluorohexanoate	PFHxA	18.4	3.5
Perfluoroheptanoate	PFHpA	6.6	3.9
Perfluorooctanoate	PFOA	21.6	3.6
Perfluoropropanesulfonate	PFPrS	3.3	1.1
Perfluorobutanesulfonate	PFBS	2.4	0.4
Perfluoropentanesulfonate	PFPeS	9.4	2.0
Perfluorohexanesulfonate	PFHxS	42.0	7.6
Perfluoroheptanesulfonate	PFHpS	1.2	0.3
Perfluorooctanesulfonate	PFOS	50.6	16.3

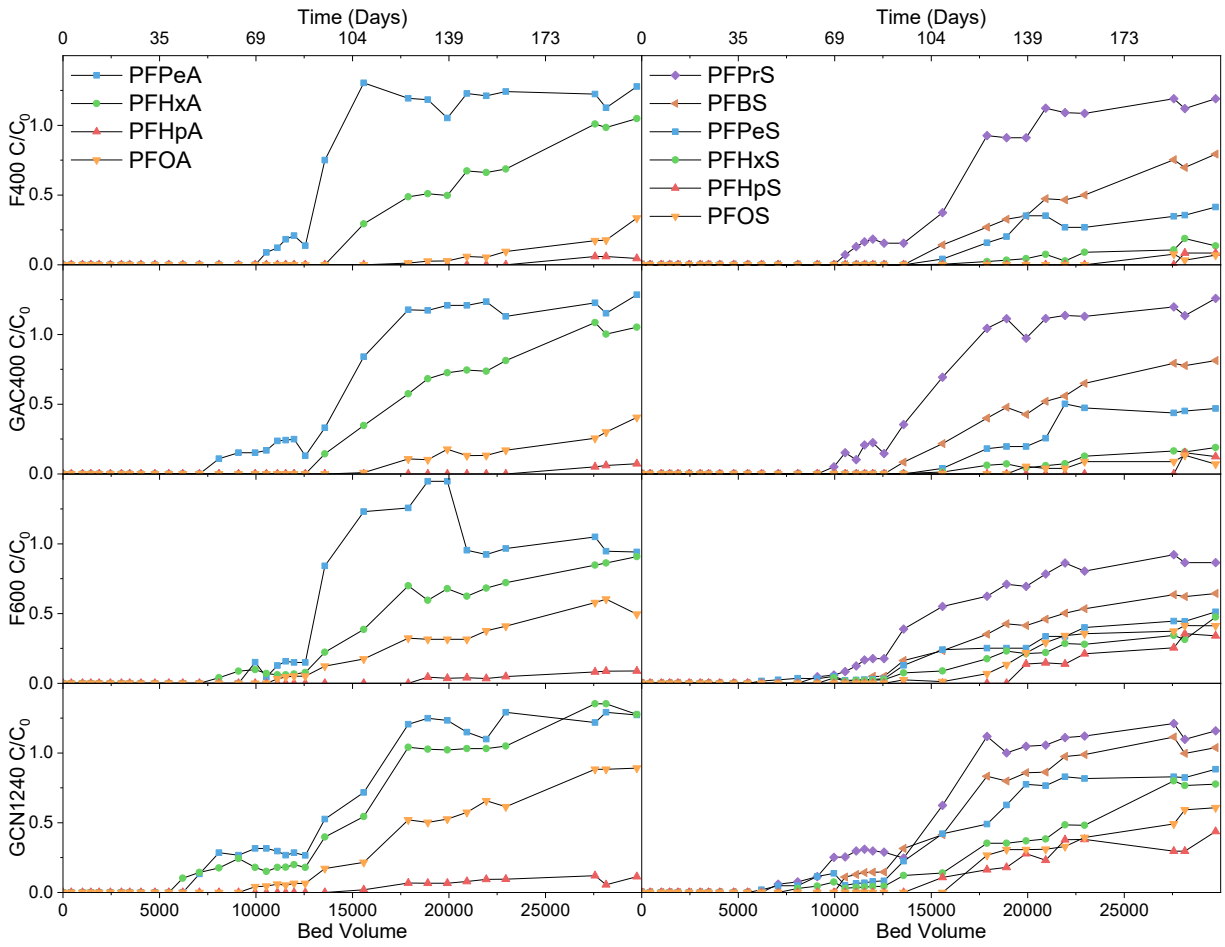

Figure 1. Breakthrough curves showing C/C_0 of each carbon verses bed volumes for four commercially available carbons with a continuous feed of PFAS contaminated groundwater. Left column shows PFCA breakthrough and right column shows PFSA breakthrough. In general, chain length dependent breakthrough is observed for all carbons.

Despite the differences in influent concentration and water matrix effects, chain length dependent breakthrough was generally observed where longer chain compounds, or more hydrophobic compounds, broke through later than shorter, or less hydrophobic compounds. As chain length increases, hydrophobicity increases as represented by increasing log K_{oc} values[49]. PFHpA and PFHpS were exceptions to this trend, which is addressed below. Chain length dependent

breakthrough was also observed in other studies with multiple PFASs[18, 20, 24, 28]. Shorter chain or weaker adsorbing compounds are expected to break through faster because of lower van der Waals hydrophobic adsorbing forces[50]. Shorter chain PFASs may also be easily displaced and desorbed by stronger adsorbing PFASs or DOC resulting in faster breakthrough[38, 51]. Desorption of shorter chain compounds like PFPeA and PFPrS is corroborated by a C/C_0 greater than 1 towards the end of the breakthrough curve. On the other hand, longer chain PFASs adsorb more strongly and are less easily displaced resulting in later breakthrough.

The later breakthrough of PFHpA and PFHpS compared to PFOA and PFOS, respectively, may be due to the presence of specific sorption sites that are the most energetically favorable for PFHpA and PFHpS sorption compared to other PFASs, or sorption sites that stronger adsorbing compounds like PFOA or PFOS cannot access due to steric effects. The combination of favorable sorption sites for PFHpA and PFHpS and the low influent concentrations of PFHpA and PFHpS may therefore result in later breakthrough. Future research is needed to investigate the influence of different influent concentrations on breakthrough performance of GAC.

3.2 Carbon Comparisons

A comparison between the masses of PFASs adsorbed at 5% breakthrough ($C/C_0 = 0.05$) is shown in Figure 2. C_0 values used were averaged influent concentrations. For shorter chain compounds like PFPeA, PFPrS, and PFBS, the mass adsorbed at breakthrough is about the same, suggesting that carbon type may not play a significant role in adsorption for these shorter chain compounds. However, as chain length increases, F400 and GAC400 significantly outperformed F600 and GCN1240 by 40-50% in mass absorbed at breakthrough for longer chain compounds like PFHxA,

PFOA, PFPeS, PFHxS, and PFOS. This may be due to the high volumes of transport pores in F400 (0.22 cm^3/g) and GAC400 (0.25 cm^3/g) compared to F600 (0.13 cm^3/g) and GCN1240 (0.12 cm^3/g). Mass transport of contaminants in GAC follows four steps: bulk solution transport, film resistance to transport, intraparticle transport, and adsorption[39, 52]. Transport pores, or presence of mesopores and macropores, have been implicated as an important factor for effective PFAS removal, especially for longer chain PFASs. This is likely due to faster diffusion through larger pores and therefore less limitations from intraparticle diffusion resulting in better utilization of sorption surface area and a better performing carbon[18, 19]. On the other hand, carbon type appeared to matter less for shorter chain compounds likely because these compounds experience less intraparticle diffusion limitations and consequentially, are less affected by the presence of transport pores.

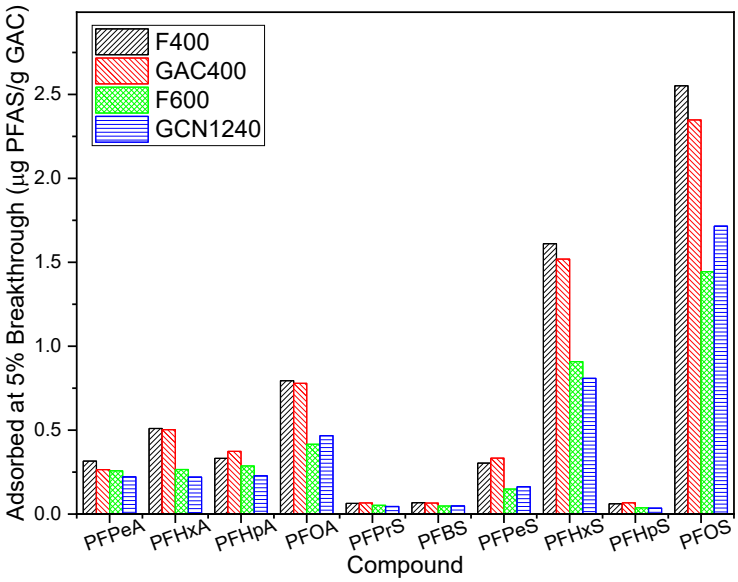

Figure 2. Adsorbed PFAS mass per gram of carbon at 5% breakthrough for all carbons tested. F400 and GAC400 appear to perform better than F600 and GCN1240 for longer chain PFASs likely due to a higher percentage of transport pores. However, for shorter chain compounds, carbon type appears to matter less.

BET surface area may also affect carbon performance. The percentage of transport pores for the bituminous coal carbons F400, GAC400, and surprisingly a poorer performing carbon, F600, are about the same at 81%, 83%, and 81%, respectively. However, because F600 has the lowest surface area of the three, the overall concentration of transport pores and consequentially, the overall available adsorption area may be less resulting in poor performance. GCN1240 on the other hand has the highest BET surface area but has the lowest percentage of transport pores at 57% percent, likely rendering a significant portion of surface area unused for PFAS adsorption because of intraparticle diffusion limitations. In fact, coconut carbons like GCN1240 are inherently microporous[52] and may not be ideal for sorption of larger contaminants like PFASs.

Sulfonates, especially longer chain sulfonates, appear to adsorb more than carboxylates prior to breakthrough. Batch studies have also corroborated these observations by finding PFOS to have a higher adsorbability than PFOA[19, 21, 29]. The difference in adsorption between PFOS and PFOA may be largely due to PFOS being more hydrophobic than PFOA given the additional perfluorinated C on PFOS. It has also been suggested that PFOS may adsorb more than PFOA because of possible hemimicelle formation within the carbon pores. Hemimicelles may form at 0.001-0.01 of the critical micelle concentration (cmc)[53] and the predicted cmc for PFOS is 4573 mg/L and 15,696 mg/L for PFOA[21]. Despite the low influent concentrations of PFOS in this study (55.7 ± 21.3 ng/L), the system was operated for seven months and the total mass accumulated over time within the carbon increases the possibility of hemimicelle formation. Although unexplored, it may also be possible that other long chain PFASs may contribute to formation of a heterogenous micelle composed of many different PFASs.

277

278 *3.4 Modeling*

279 Column breakthrough curves were fit with a solid liquid partition coefficient (K_d) by minimizing
280 the sum of the squared residuals (SSR) using two models: an instantaneous sorption equilibrium
281 model and an intraparticle diffusion model. The intraparticle diffusion model includes a tortuosity
282 (τ) term which cannot be directly measured and is typically estimated through theoretical
283 approaches. However, many of these theoretical approaches rely on unrealistic ideal geometries[54,
284 55]. If tortuosity is not estimated through these theoretical approaches, it is then used as an adjustable
285 factor in model fits and may not bear any meaning pertaining to specific sorbates or sorbents[54].
286 Tortuosity has been indirectly measured by studies with activated carbon showing values ranging
287 between 1 and 6[56, 57]. Figure S3 and Table S8 in the ESI show the results of changing tortuosity at
288 the same K_d value for the intraparticle diffusion model; as tortuosity increases, the fit was worse
289 and the SSR increased. Therefore, due to the uncertainties associated with tortuosity, an unbiased
290 best-case fit with a value of $\tau = 1$ was chosen for the sake of comparison between the models.

291

292 The equilibrium model assumes instantaneous sorption equilibrium and no diffusion limitations
293 between the sorbent and sorbate. The intraparticle diffusion model assumes non-equilibrium
294 sorption conditions due to intraparticle diffusion limitations, typically resulting in breakthrough
295 curves influenced by fronting and tailing[47]. Fronting is early breakthrough of compounds due to
296 incomplete equilibrium between sorbent and sorbate during the column passage, which may be
297 due to slow intraparticle diffusion hindering access to sorption sites within the core of the GAC
298 particles[58]. Similarly, tailing is primarily due to incomplete equilibrium between sorbent and

sorbate during the desorption process, where release of sorbate molecules from the core of the GAC particles occurs slowly and time to complete breakthrough is longer[58].

Intraparticle diffusion model fits at $\tau = 1$ and equilibrium model fits are shown in Figure 3 for one of the best performing carbons, F400, and comparisons between SSR values for both models are shown in Figure 4. Model breakthrough curve fits and K_d values for all carbons are shown in Figures S4 and S5 and summarized in Tables S6 and S7 in the ESI, respectively.

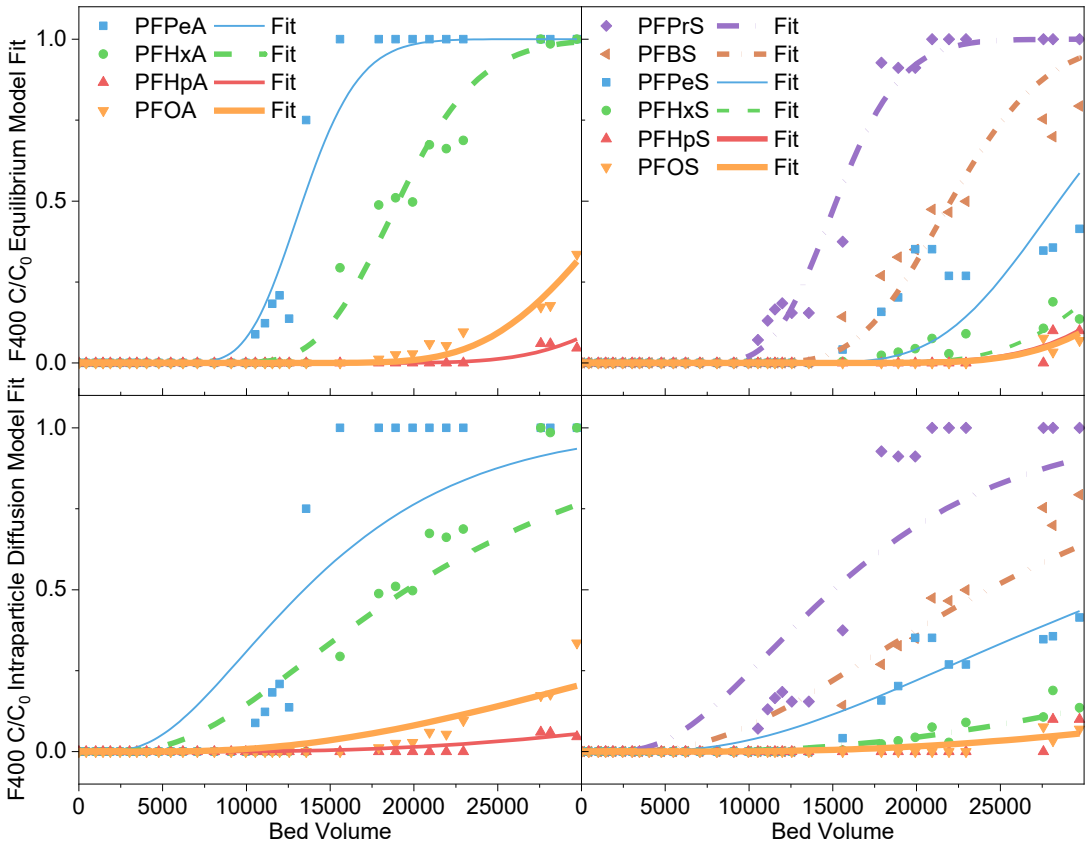

Figure 3. Model fits for one of the best performing carbons, F400. Left column shows PFCAs and right column shows PFSAs. Top row shows equilibrium model fits and bottom row shows intraparticle diffusion model fits at τ=1. While the pilot data exhibits some fronting and tailing in

311 comparison with the equilibrium model fits, the intraparticle diffusion model fits at τ=1 appear to
312 overexpress fronting and tailing.

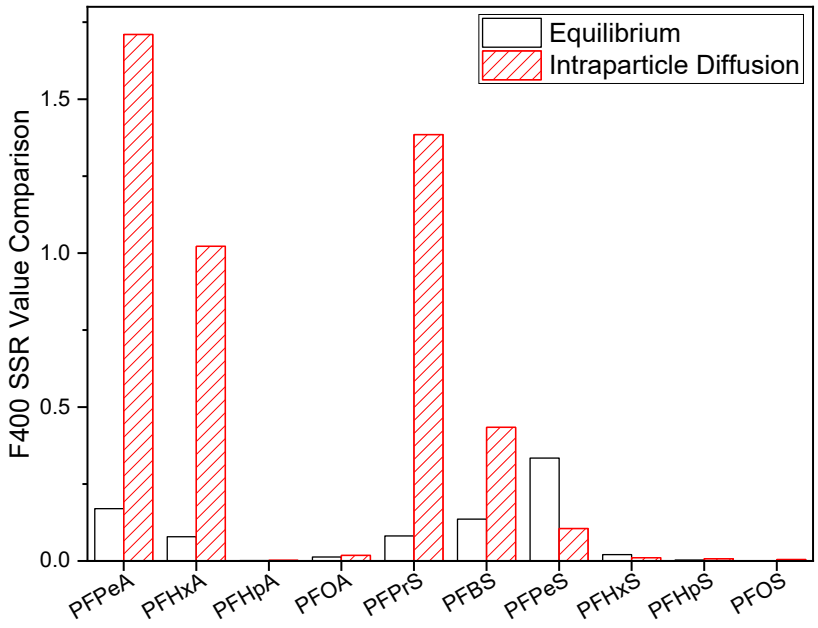

313

314 **Figure 4.** SSR comparisons between intraparticle diffusion and equilibrium model fits for F400.
315 A larger SSR value denotes a worse fit. Shorter chain compounds appear to fit the equilibrium
316 model better, while the intraparticle diffusion and equilibrium models appear to fit longer chain
317 compounds equally well.

318

319 The equilibrium model fit breakthrough data for shorter chain and weakly adsorbing compounds
320 like PFPeA, PFHxS, PFPrS, and PFBS better than the intraparticle diffusion model as shown in
321 Figures 3 and 4. This may be because these compounds are less affected by intraparticle diffusion
322 limitations resulting in a faster time to equilibrium. For longer chain and strongly adsorbing
323 compounds like PFHpA, PFOA, PFHxS, PFHpS, and PFOS, both equilibrium and intraparticle
324 diffusion models appear to fit breakthrough data well. Intraparticle diffusion effects are still
325 somewhat relevant as evidenced by some fronting and tailing in comparison with equilibrium

model fits. However, the intraparticle diffusion model appears to overexpress fronting and tailing in the model fit. It has been previously reported based on concentration profiles measured within GAC particles, that GAC macropores enable faster intraparticle diffusion than shown by the intraparticle diffusion model[59]. Water matrix effects like DOC may also influence model fits. DOC may reduce sorption capacity leading to faster breakthrough, resulting in less fronting and tailing and better fits to the equilibrium model. Another explanation may be because complete breakthrough was not observed for some PFASs, and model fits may change with complete breakthrough.

The model fitting trends were similar for other carbons as well. The difference between the intraparticle diffusion model SSR values and equilibrium model SSR values are shown in Figure 5. Because a higher SSR value denotes a worse fit, a positive difference between the intraparticle diffusion model SSR and equilibrium model SSR means a stronger fit for the equilibrium model while a negative difference means a stronger fit for the intraparticle diffusion model.

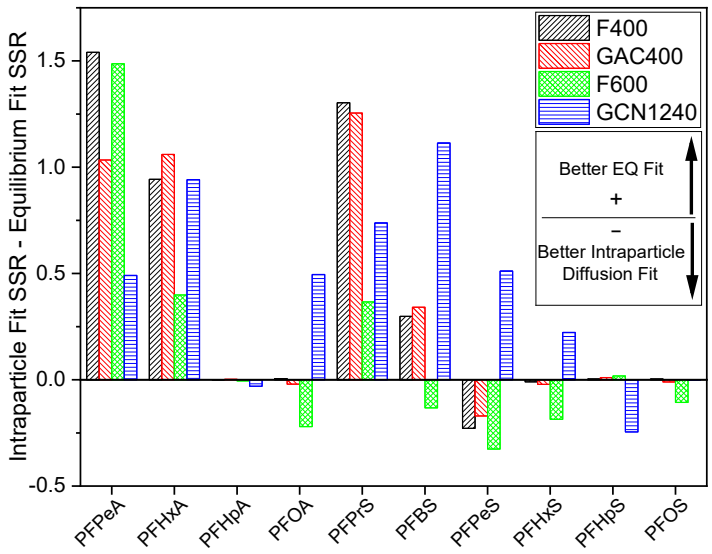

Figure 5. Difference between intraparticle diffusion model SSR and equilibrium model SSR. Positive values indicate stronger equilibrium model fits and negative values indicate stronger intraparticle diffusion model fits. Across all carbons, in general, the equilibrium model appears to fit shorter chain compounds better than the intraparticle diffusion model. For longer chain compounds, in general, the equilibrium and intraparticle diffusion models appear to fit equally as well. The equilibrium model may be a better and more practical model fit.

Despite a few outliers, the equilibrium model in general, fits the data as well as, if not better than the intraparticle diffusion model for all carbons and PFASs present in the influent. The equilibrium model may also be a more practical modeling approach for practitioner purposes. This is because the equilibrium model inherently includes a safety factor by reaching GAC exhaustion faster than shown by the pilot breakthrough data, while the intraparticle diffusion model expresses GAC exhaustion slower than the pilot breakthrough data. Lastly, the equilibrium model may also be more advantageous than the intraparticle diffusion model due to model simplicity and fewer fitting parameters.

Comparisons and Practical Implications

Xiao et al. 2017[20] determined K_d values from small batch-scale tests using a microporous carbon[60, 61], the Calgon Filtrasorb 300 (F300), a carbon not tested in this study. A comparison between K_d values determined from F300 batch studies verses the K_d values determined for all carbons tested in this study from the equilibrium model fit of pilot-scale data is provided in Figure 6. In general, the K_d values from the batch study are smaller for shorter chain compounds and larger for longer chain compounds compared to the K_d values from the equilibrium model fit. This suggests that

364 batch derived K_d values may predict a longer time to breakthrough, or larger adsorption capacity,
365 for longer chain compounds and a shorter time to breakthrough, or smaller adsorption capacity,
366 for shorter chain compounds. This may not be ideal, especially for longer chain compounds like
367 PFOA and PFOS which are under health advisories.
368
369 The differences between observed K_d values from batch and pilot studies may be due to DOC.
370 Although a high DOC concentration of 46 mg/L was used in the batch study with F300[20], GAC in
371 flow-through column studies with a continuous source of groundwater is exposed to significantly
372 higher DOC masses over time suggesting that batch studies may not accurately represent the
373 impact of DOC on adsorption. In addition, potential GAC fouling by biofilms and solid precipitates
374 may also influence GAC performance to a greater degree at the pilot-scale than at batch-scale.
375
376 Practitioners could estimate breakthrough of PFASs using the equilibrium model by inputting
377 different PFAS feed concentrations, system constants described in Table S2, and by using the
378 derived K_d values from the equilibrium model fits provided in this study. While neither the
379 equilibrium nor intraparticle diffusion models allow for water quality inputs, the derived K_d values
380 inherently include impacts of water quality on PFAS breakthrough with GAC. However,
381 predictions may only be accurate for similar water qualities. For PFASs not included in this study,
382 K_d values can be interpreted from a linear regression relationship relating chain length verses K_d
383 for both models in Tables S9 and S10.

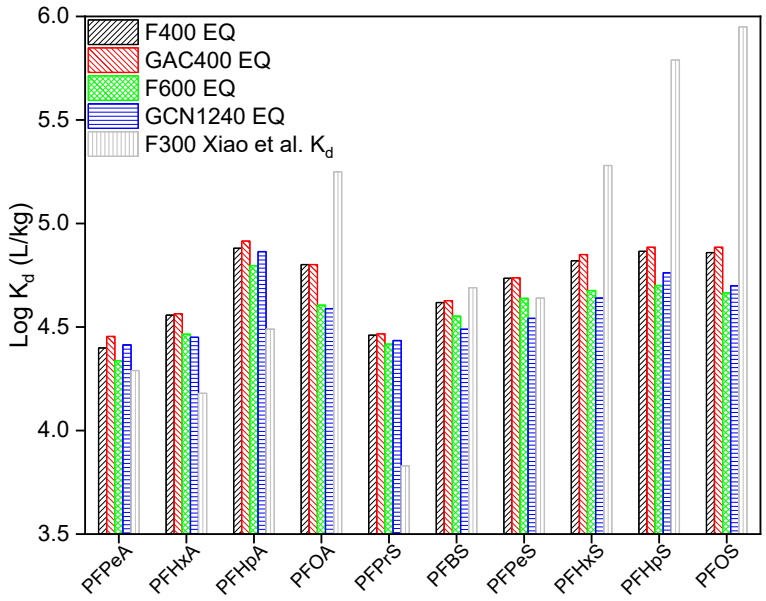

Figure 6. Comparisons between equilibrium model K_d values for all GACs and batch study K_d values for F300 from Xiao et al 2017[20]. In general, the K_d values from the F300 batch study are larger for longer chain compounds and smaller for shorter chain compounds compared to the K_d values for the pilot study.

Conclusions and Implications

GAC breakthrough was observed for 10 different PFASs using contaminated groundwater through a 7-month long pilot-scale system comparing four commercially available activated carbons. In general, chain length dependent breakthrough was observed with exceptions for PFHpA and PFHpS. The non-chain length dependent breakthrough behavior of PFHpA and PFHpS may be due to a combination of low influent concentrations and favorable sorption sites. Carbon type appeared to matter less for shorter chain compounds; however, F400 and GAC400 performed 40-50% better than F600 and GCN1240 for longer chain compounds most likely due to higher percentages of transport pores resulting in less intraparticle diffusion limitations. Pilot-scale breakthrough results were fitted with two models: an equilibrium and an intraparticle diffusion

model. The equilibrium model was found to provide a better fit to the breakthrough data and to be a more practical model. Comparing K_d values between equilibrium model fits and a separate batch study showed differences in K_d values, which may have been influenced by experimental differences between batch-scale and pilot-scale. The results and modeling efforts of this pilot-scale study using a using a continuous source of real contaminated water therefore provides a better understanding of real world GAC PFAS breakthrough behavior for future academic studies, practitioners, and regulators. Future studies should continue to investigate the impact of different water matrices, especially varying concentrations of DOC, and varying influent concentrations of different PFASs on GAC breakthrough using real water in column studies. A comprehensive library of K_d values representative of a wide and diverse range of water matrices can then be derived from these studies to provide better guidance for practitioners using GAC to remove PFASs.

Conflict of Interest Statement

There are no conflicts of interest to declare.

Acknowledgements

The authors would like to thank the City of Fountain, Colorado for funding this research. Special thanks to Michael Fink (City of Fountain Water Superintendent) and City of Fountain Utilities, especially Justin Moore and Jasson Palmer; to Tzahi Cath, Mike Veres, and Tani Cath for their assistance in designing and fabricating the pilot system; to Kate Spangler and Estefani Bustos for their assistance in water quality analysis; to Timothy Strathmann for his advice; to Alyssa Hodgin for investigating breakthrough of XIC library compounds; to Brian Trewyn's lab and

Conner Murray for their assistance in carbon characterization; to Bridget Ulrich for her initial input on transport modeling; to Tzahi Cath and Garrett Mckay for their revisions; to Calgon Carbon Corporation for providing carbon for the research, especially Richard Mimna; to Cabot Norit Corporation for providing carbon for the research.

References

1. K. A. Barzen-Hanson, S. C. Roberts, S. Choyke, K. Oetjen, A. McAlees, N. Riddell, R. McCrindle, P. L. Ferguson, C. P. Higgins and J. A. Field, Discovery of 40 Classes of Per- and Polyfluoroalkyl Substances in Historical Aqueous Film-Forming Foams (AFFFs) and AFFF-Impacted Groundwater, *Environ Sci Technol*, 2017, **51**, 2047-2057.

2. S. R. de Solla, A. O. De Silva and R. J. Letcher, Highly elevated levels of perfluorooctane sulfonate and other perfluorinated acids found in biota and surface water downstream of an international airport, Hamilton, Ontario, Canada, *Environ Int*, 2012, **39**, 19-26.

3. E. F. Houtz, C. P. Higgins, J. A. Field and D. L. Sedlak, Persistence of perfluoroalkyl acid precursors in AFFF-impacted groundwater and soil, *Environ Sci Technol*, 2013, **47**, 8187-8195.

4. X. C. Hu, D. Q. Andrews, A. B. Lindstrom, T. A. Bruton, L. A. Schaider, P. Grandjean, R. Lohmann, C. C. Carignan, A. Blum, S. A. Balan, C. P. Higgins and E. M. Sunderland, Detection of Poly- and Perfluoroalkyl Substances (PFASs) in U.S. Drinking Water Linked to Industrial Sites, Military Fire Training Areas, and Wastewater Treatment Plants, *Environmental Science & Technology Letters*, 2016, **3**, 344-350.

5. K. Kannan, S. Corsolini, J. Falandysz, G. Fillmann, K. S. Kumar, B. G. Loganathan, M. A. Mohd, J. Olivero, N. Van Wouwe, J. H. Yang and K. M. Aldous, Perfluorooctanesulfonate and related fluorochemicals in human blood from several countries, *Environ. Sci. Technol.*, 2004, **38**, 4489-4495.

6. C. Kunacheva, S. Fujii, S. Tanaka, S. T. Seneviratne, N. P. Lien, M. Nozoe, K. Kimura, B. R. Shivakoti and H. Harada, Worldwide surveys of perfluorooctane sulfonate (PFOS) and perfluorooctanoic acid (PFOA) in water environment in recent years, *Water Sci Technol*, 2012, **66**, 2764-2771.

7. P. Rostkowski, N. Yamashita, I. M. Ka So, S. Taniyasu, P. K. S. Lam, J. Falandysz, K. T. Lee, S. K. Kim, J. S. Khim, S. H. Im, J. L. Newsted, P. D. Jones, K. Kannan and J. P. Giesy, PERFLUORINATED COMPOUNDS IN STREAMS OF THE SHIHWA INDUSTRIAL ZONE AND LAKE SHIHWA, SOUTH KOREA, *Environmental Toxicology and Chemistry*, 2006, **25**, 2374.

8. D. O'Hagan, Understanding organofluorine chemistry. An introduction to the C-F bond, *Chem Soc Rev*, 2008, **37**, 308-319.

9. USEPA, Drinking Water Health Advisory for Perfluorooctanoic Acid (PFOA).*Journal*, 2016.

10. USEPA, Drinking Water Health Advisory for Perfluorooctane Sulfonate (PFOS).*Journal*, 2016.

11. M. Ghisari, H. Eiberg, M. Long and E. C. Bonefeld-Jørgensen, Polymorphisms in Phase I and Phase II genes and breast cancer risk and relations to persistent organic pollutant exposure: a case–control study in Inuit women, *Environmental Health*, 2014, **13**, 19.

12. P. Grandjean and R. Clapp, Perfluorinated Alkyl Substances, *NEW SOLUTIONS: A Journal of Environmental and Occupational Health Policy*, 2015, **25**, 147-163.

13. X. Li, J. Ma, G. Liu, J. Fang, S. Yue, Y. Guan, L. Chen and X. Liu, Efficient Reductive Dechlorination of Monochloroacetic Acid by Sulfite/UV Process, *Environ. Sci. Technol.*, 2012, **46**, 7342-7349.

14. Y. Qian, X. Guo, Y. Zhang, Y. Peng, P. Sun, C.-H. Huang, J. Niu, X. Zhou and J. C. Crittenden, Perfluorooctanoic Acid Degradation Using UV–Persulfate Process: Modeling of the Degradation and Chlorate Formation, 2016, **50**, 772-781.

15. R. K. Singh, S. Fernando, S. Fakouri Baygi, N. Multari, S. Mededovic Thagard and T. M. Holsen, Breakdown products from perfluorinated alkyl substances (PFAS) degradation in a plasma-based water treatment process, *Environ. Sci. Technol.*, 2019, DOI: 10.1021/acs.est.8b07031.

16. E. Steinle-Darling and M. Reinhard, Nanofiltration for trace organic contaminant removal: Structure, solution, and membrane fouling effects on the rejection of perfluorochemicals, *Environ. Sci. Technol.*, 2008, **42**, 5292-5297.

17. C. Y. Y. Tang, Q. S. Fu, A. P. Robertson, C. S. Criddle and J. O. Leckie, Use of reverse osmosis membranes to remove perfluorooctane sulfonate (PFOS) from semiconductor wastewater, *Environ. Sci. Technol.*, 2006, **40**, 7343-7349.

18. T. D. Appleman, E. R. Dickenson, C. Bellona and C. P. Higgins, Nanofiltration and granular activated carbon treatment of perfluoroalkyl acids, *J Hazard Mater*, 2013, **260**, 740-746.

19. S. Deng, Y. Nie, Z. Du, Q. Huang, P. Meng, B. Wang, J. Huang and G. Yu, Enhanced adsorption of perfluorooctane sulfonate and perfluorooctanoate by bamboo-derived granular activated carbon, *J Hazard Mater*, 2015, **282**, 150-157.

20. X. Xiao, B. A. Ulrich, B. Chen and C. P. Higgins, Sorption of Poly- and Perfluoroalkyl Substances (PFASs) Relevant to Aqueous Film-Forming Foam (AFFF)-Impacted Groundwater by Biochars and Activated Carbon, *Environ Sci Technol*, 2017, **51**, 6342-6351.

21. Q. Yu, R. Zhang, S. Deng, J. Huang and G. Yu, Sorption of perfluorooctane sulfonate and perfluorooctanoate on activated carbons and resin: Kinetic and isotherm study, *Water Res*, 2009, **43**, 1150-1158.

22. D. Zhang, Q. Luo, B. Gao, S. Y. Chiang, D. Woodward and Q. Huang, Sorption of perfluorooctanoic acid, perfluorooctane sulfonate and perfluoroheptanoic acid on granular activated carbon, *Chemosphere*, 2016, **144**, 2336-2342.

23. S. Deng, Q. Yu, J. Huang and G. Yu, Removal of perfluorooctane sulfonate from wastewater by anion exchange resins: Effects of resin properties and solution chemistry, *Water Res.*, 2010, **44**, 5188-5195.

24. P. McCleaf, S. Englund, A. Ostlund, K. Lindegren, K. Wiberg and L. Ahrens, Removal efficiency of multiple poly- and perfluoroalkyl substances (PFASs) in drinking water using granular activated carbon (GAC) and anion exchange (AE) column tests, *Water Res*, 2017, **120**, 77-87.

25. A. Zaggia, L. Conte, L. Falletti, M. Fant and A. Chiorboli, Use of strong anion exchange resins for the removal of perfluoroalkylated substances from contaminated drinking water in batch and continuous pilot plants, *Water Res.*, 2016, **91**, 137-146.

26. S. T. Senevirathna, S. Tanaka, S. Fujii, C. Kunacheva, H. Harada, B. R. Shivakoti and R. Okamoto, A comparative study of adsorption of perfluorooctane sulfonate (PFOS) onto granular activated carbon, ion-exchange polymers and non-ion-exchange polymers, *Chemosphere*, 2010, **80**, 647-651.

27. M. F. Rahman, S. Peldszus and W. B. Anderson, Behaviour and fate of perfluoroalkyl and polyfluoroalkyl substances (PFASs) in drinking water treatment: a review, *Water Res*, 2014, **50**, 318-340.

28. D. N. Kothawala, S. J. Kohler, A. Ostlund, K. Wiberg and L. Ahrens, Influence of dissolved organic matter concentration and composition on the removal efficiency of perfluoroalkyl substances (PFASs) during drinking water treatment, *Water Res*, 2017, **121**, 320-328.

29. V. Ochoa-Herrera and R. Sierra-Alvarez, Removal of perfluorinated surfactants by sorption onto granular activated carbon, zeolite and sludge, *Chemosphere*, 2008, **72**, 1588-1593.

30. C. J. Corwin and R. S. Summers, Adsorption and desorption of trace organic contaminants from granular activated carbon adsorbers after intermittent loading and throughout backwash cycles, *Water Res*, 2011, **45**, 417-426.

31. S. Hong and R. S. Summers, Effect of backwashing on activated carbon adsorption using plug flow pore surface diffusion model, *Korean J. Chem. Eng.*, 2006, **23**, 57-62.

32. P. C. To, B. J. Mariñas, V. L. Snoeyink and W. J. Ng, Effect of Pore-Blocking Background Compounds on the Kinetics of Trace Organic Contaminant Desorption from Activated Carbon, *Environ. Sci. Techno*, 2008, **42**, 4825-4830.

33. P. C. To, B. J. Mariñas, V. L. Snoeyink and W. J. Ng, Effect of Strongly Competing Background Compounds on the Kinetics of Trace Organic Contaminant Desorption from Activated Carbon, *Environ. Sci. Techno*, 2008, **42**, 2606-2611.

34. K. Ebie, F. Li, Y. Azuma, A. Yuasa and T. Hagishita, Pore distribution effect of activated carbon in adsorbing organic micropollutants from natural water, *Water Res*, 2001, **35**, 167-179.

35. C. J. Corwin and R. S. Summers, Scaling Trace Organic Contaminant Adsorption Capacity by Granular Activated Carbon, *Environ. Sci. Techno*, 2010, **44**, 5403-5408.

36. D. R. U. Knappe, V. L. Snoeyink, P. Roche, M. J. Prados and M.-M. Bourbigot, Atrazine removal by preloaded GAC, *Journal - American Water Works Association*, 1999, **91**, 97-109.

37. R. S. Summers, S. M. Kim, K. Shimabuku, S.-H. Chae and C. J. Corwin, Granular activated carbon adsorption of MIB in the presence of dissolved organic matter, *Water Res*, 2013, **47**, 3507-3513.

38. C. Eschauzier, E. Beerendonk, P. Scholte-Veenendaal and P. De Voogt, Impact of Treatment Processes on the Removal of Perfluoroalkyl Acids from the Drinking Water Production Chain, *Environ. Sci. Techno*, 2012, **46**, 1708-1715.

39. J. K. Edzwald, *Water Quality & Treatment: A Handbook on Drinking Water*, American Water Works Association, Denver, Colorado, 6th edn., 2011.

40. M. C. Carter and W. J. Weber, Modeling Adsorption of TCE by Activated Carbon Preloaded by Background Organic Matter, *Environ. Sci. Techno*, 1994, **28**, 614-623.

41. J. C. Crittenden, P. S. Reddy, D. W. Hand and H. Arora, *Prediction of GAC Performance Using Rapid Small-Scale Column Tests, AWWARF report #90549*, American Water Works Association, Denver, CO, 1989.

42. C. C. Murray, H. Vatankhah, C. A. McDonough, A. Nickerson, T. T. Hedtke, T. Y. Cath, C. P. Higgins and C. L. Bellona, Removal of per- and polyfluoroalkyl substances using super-fine powder activated carbon and ceramic membrane filtration, *J Hazard Mater*, 2018, **366**, 160-168.

43. I. Ericson, J. L. Domingo, M. Nadal, E. Bigas, X. Llebaria, B. Van Bavel and G. Lindström, Levels of Perfluorinated Chemicals in Municipal Drinking Water from Catalonia, Spain: Public Health Implications, *Arch Environ Contam Toxicol* 2009, **57**, 631-638.

44. G. B. Post, J. B. Louis, K. R. Cooper, B. J. Boros-Russo and R. L. Lippincott, Occurrence and Potential Significance of Perfluorooctanoic Acid (PFOA) Detected in New Jersey Public Drinking Water Systems, *Environ. Sci. Techno*, 2009, **43**, 4547-4554.

45. S. Takagi, F. Adachi, K. Miyano, Y. Koizumi, H. Tanaka, I. Watanabe, S. Tanabe and K. Kannan, Fate of Perfluorooctanesulfonate and perfluorooctanoate in drinking water treatment processes, *Water Res*, 2011, **45**, 3925-3932.

46. Z. Yu, S. Peldszus and P. M. Huck, Adsorption characteristics of selected pharmaceuticals and an endocrine disrupting compound—Naproxen, carbamazepine and nonylphenol—on activated carbon, *Water Res.*, 2008, **42**, 2873-2882.

47. D. Werner, H. K. Karapanagioti and D. A. Sabatini, Assessing the effect of grain-scale sorption rate limitations on the fate of hydrophobic organic groundwater pollutants, *J Contam Hydrol*, 2012, **129-130**, 70-79.

48. L. Ahrens, K. Norström, T. Viktor, A. P. Cousins and S. Josefsson, Stockholm Arlanda Airport as a source of per- and polyfluoroalkyl substances to water, sediment and fish, *Chemosphere*, 2015, **129**, 33-38.

49. H. Campos Pereira, M. Ullberg, D. B. Kleja, J. P. Gustafsson and L. Ahrens, Sorption of perfluoroalkyl substances (PFASs) to an organic soil horizon – Effect of cation composition and pH, *Chemosphere*, 2018, **207**, 183-191.

50. J. C. Crittenden, R. R. Trussell, D. W. Hand, K. J. Howe and G. Tchobanoglous, *MWH's Water Treatment Principles and Design*, John Wiley & Sons, Inc., Hoboken, New Jersey, 3rd edn., 2012.

51. C. p. Higgins and R. g. Luthy, Sorption of Perfluorinated Surfactants on Sediments, *Environ. Sci. Technol*, 2006, **40**, 7251-7256.

52. Z. K. Chowdhury, R. S. Summers, G. P. Westerhoff, B. J. Leto, K. O. Nowack, C. J. Corwin and L. B. Passantino, *Activated Carbon: Solutions for Improving Water Quality*, 2013.

53. R. P. Schwarzenbach, P. M. Gschwend and D. M. Imboden, *Environmental Organic Chemistry*, John Wiley & Sons, Inc., Hoboken, New Jersey, 2nd edn., 2003.

54. B. Ghanbarian, A. G. Hunt, R. P. Ewing and M. Sahimi, Tortuosity in Porous Media: A Critical Review, *Soil Science Society of America Journal*, 2013, **77**, 1461-1477.

55. L. Shen and Z. Chen, Critical review of the impact of tortuosity on diffusion, *Chemical Engineering Science*, 2007, **62**, 3748-3755.

56. J.-Y. San, Y.-C. Hsu and L.-J. Wu, Adsorption of toluene on activated carbon in a packed bed, *International Journal of Heat and Mass Transfer*, 1998, **41**, 3229-3238.

57. R. Ocampo-Pérez, M. M. Abdel Daiem, J. Rivera-Utrilla, J. D. Méndez-Díaz and M. Sánchez-Polo, Modeling adsorption rate of organic micropollutants present in landfill leachates onto granular activated carbon, *Journal of Colloid and Interface Science*, 2012, **385**, 174-182.

58. P. Grathwohl, *DIFFUSION IN NATURAL POROUS MEDIA: Contaminant Transport, Sorption/Desorption and Dissolution Kinetics*, Springer Science + Business Media, LLC, New York, 1998.

590 59. S. Ahn, D. Werner, H. K. Karapanagioti, D. R. McGlothlin, R. N. Zare and R. G. Luthy,
591 Phenanthrene and pyrene sorption and intraparticle diffusion in polyoxymethylene, coke, and
592 activated carbon, *Environ. Sci. Technol.*, 2005, **39**, 6516-6526.

593 60. C.-T. Hsieh and H. Teng, Influence of mesopore volume and adsorbate size on adsorption
594 capacities of activated carbons in aqueous solutions, *Carbon*, 2000, **38**, 863-869.

595 61. B. A. Ulrich, E. A. Im, D. Werner and C. P. Higgins, Biochar and activated carbon for enhanced
596 trace organic contaminant retention in stormwater infiltration systems, *Environ Sci Technol*,
597 2015, **49**, 6222-6230.
598